analytical chemistry

Article

pubs.acs.org/ac

Dopant-Assisted Negative Photoionization Ion Mobility Spectrometry for Sensitive Detection of Explosives

Shasha Cheng,[†,‡] Jian Dou,[§] Weiguo Wang,[†] Chuang Chen,[†,‡] Lei Hua,[†] Qinghua Zhou,[†,‡] Keyong Hou,[†] Jinghua Li,[†] and Haiyang Li*[,†]

[†]Dalian Institute of Chemical Physics, Chinese Academy of Sciences, Dalian, 116023, People's Republic of China

[‡]Graduate University of Chinese Academy of Sciences, Beijing, 100049, People's Republic of China

[§]Department of Instrumentation & Electrical Engineering, Jilin University, Jilin, 130021, People's Republic of China

Supporting Information

ABSTRACT: Ion mobility spectrometry (IMS) is a key trace detection technique for explosives and the development of a simple, stable, and efficient nonradioactive ionization source is highly demanded. A dopant-assisted negative photoionization (DANP) source has been developed for IMS, which uses a commercial VUV krypton lamp to ionize acetone as the source of electrons to produce negative reactant ions in air. With 20 ppm of acetone as the dopant, a stable current of reactant ions of 1.35 nA was achieved. The reactant ions were identified to be $CO_3^-(H_2O)_n$ (K_0 = 2.44 cm^2 V^{-1} s^{-1}) by atmospheric pressure time-of-flight mass spectrometry, while the reactant ions in ^{63}Ni source were $O_2^-(H_2O)_n$ (K_0 = 2.30 cm^2 V^{-1} s^{-1}). Finally, its capabilities for detection of common explosives including ammonium nitrate fuel oil (ANFO), 2,4,6-trinitrotoluene (TNT), *N*-nitrobis(2-hydroxyethyl)amine dinitrate (DINA), and pentaerythritol tetranitrate (PETN) were evaluated, and the limits of detection of 10 pg (ANFO), 80 pg (TNT), and 100 pg (DINA) with a linear range of 2 orders of magnitude were achieved. The time-of-flight mass spectra obtained with use of DANP source clearly indicated that PETN and DINA can be directly ionized by the ion-association reaction of CO_3^- to form PETN·CO_3^- and DINA·CO_3^- adduct ions, which result in good sensitivity for the DANP source. The excellent stability, good sensitivity, and especially the better separation between the reactant and product ion peaks make the DANP a potential nonradioactive ionization source for IMS.

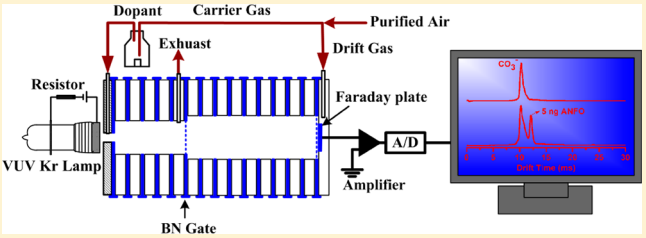

Ion mobility spectrometry (IMS) has been proved the leading technology for on-site detection of trace amounts of chemical warfare agents (CWA), explosives, narcotics, and some toxic industrial chemicals at atmospheric pressure due to its many attractive features such as high sensitivity, short response time, and comparatively low cost.[1−7] In addition, it also can provide sensitive and selective detection after separation of gas chromatography[8−11] or high-performance liquid chromatography.[12]

Ionization source is one of the most important components of an IMS instrument. The widely used ionization source in commercial IMS is ^{63}Ni source due to its simplicity, stability, long lifetime, and no need for an extra power supply.[1] However, its radioactivity restricts its application because of safety, environmental, and regulatory concerns. In recent years, many nonradioactive sources were developed as a potential substitute for ^{63}Ni source such as ultraviolet radiation photoionization,[13−16] corona discharge ionization,[17−20] electrospray ionization,[21−24] and glow discharge ionization.[25,26] Among them, ultraviolet radiation photoionization source in positive mode for ion mobility spectrometry has been well investigated due to its advantages of high selectivity and nonradioactivity.[14,27] The earliest photoionization ion mobility spectrometer was reported by the Hill group.[13] They developed a photoionization ion mobility detector for gas chromatograph working in nitrogen gas; the ionization source was made by a 10.0-eV krypton lamp mounted perpendicular to the axis of the drift tube. Eiceman et al. constructed a photoionization ion mobility spectrometer using an on-axis mounted 10.2-eV hydrogen discharge lamp in air, and ten organic compounds were detected with detection limits from 0.1 to 50 ppb and working ranges were improved 100- to 1000-fold.[14] Baumbach and Sielemann reported a membrane inlet ion mobility spectrometer (IMS) with radioactive and UV ionization sources in combination with multicapillary columns (MCCs) for real-time monitoring of methyl *tert*-butyl ether (MTBE) in water and nitrogen as well as the monoaromatic compounds benzene, toluene, and *m*-xylene (BTX).[15] Recently, Tabrizchi described an ion mobility spectrometer equipped with an atmospheric pressure photoionization and a corona discharge ionization source and observed peaks from either the corona discharge or photoionization individually or simultaneously, which makes it possible to accurately compare peaks in the ion mobility spectra

Received: September 29, 2012
Accepted: December 3, 2012
Published: December 3, 2012

   dx.doi.org/10.1021/ac302836f | *Anal. Chem.* 2013, 85, 319−326

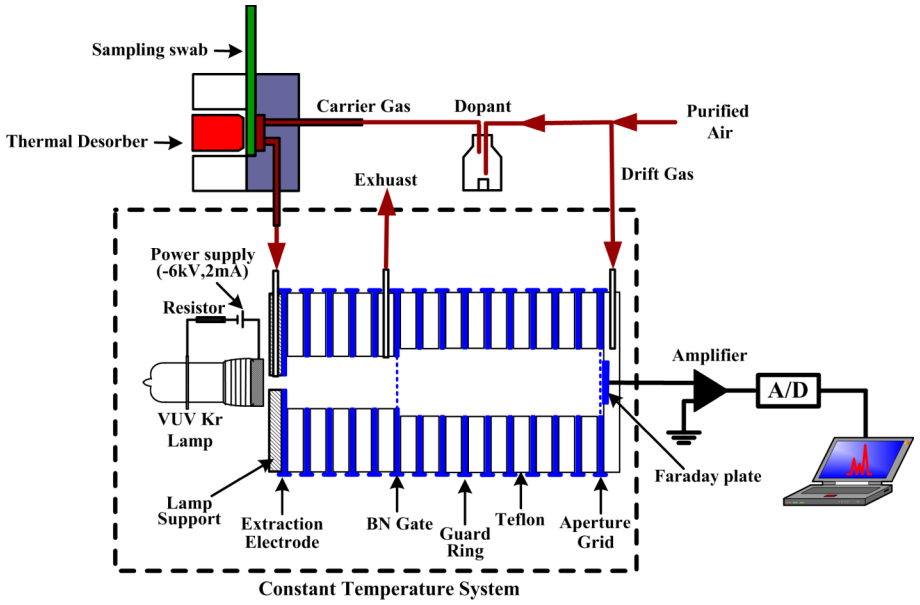

Figure 1. Schematic diagram of the dopant-assisted negative photoionization ion mobility spectrometer for sensitive detection of explosives.

from each individual source.[16] Positive photoionization ion mobility spectrometry was mostly applied in the detection of compounds with ionization potential (IP) lower than the energy of photons. Explosive compounds, such as ammonium nitrate, 2,4,6-trinitrotoluene, and pentaerythritol tetranitrate, are salts or molecules with strong electrophilic groups $-NO_2$ and $-ONO_2$, and their IPs are too high to be ionized commercially by available krypton or hydrogen discharge lamp, but they can be easily and sensitively detected by negative mode ion mobility spectrometry due to their large positive electron affinities.[1−3]

Recently, photoemissive ionization sources in negative mode for IMS have attracted much attention, in which electrons are produced by irradiating a metal surface by UV light or a laser beam. Simmonds et al. developed a photoemissive IMS by ultraviolet irradiation on a thin gold layer from a pulsed xenon lamp or low-pressure mercury lamp, and investigated the factors influencing the performance for trace detection of benzoylacetone and acetylaccetone vapor in air.[28] Walls et al. investigated the capability of a pulsed laser as UV light source for a photoemissive ion mobility spectrometer to detect trace chlorinated aliphatic compounds.[29] Previously, we developed a vacuum ultraviolet radiation induced (UVRI) negative ionization source based on photoelectric effect by irradiating the metal surface with a 10.0-eV VUV lamp.[30] UVRI was proved to be a high efficiency ionization source for explosives and some inorganic small molecules; however, its signal intensity declined gradually with the increase of running time (which can be seen in Figure 4a). The intensity decay of photoemission process was also observed by Bunker et al., and they concluded that the oxidation or coating of photocathode surface probably inhibited the electron emission.[31] The oxidation and contamination of the metal surface in a high-temperature ion mobility tube cannot be easily avoided when using air as the carrier and drift gases. The intensity decay of the photoemissive source will not only restrict its applications for on-line quantitative analysis but also increase the false alarm rate for on-site detection of explosives.

The electrons could be efficiently produced by photoionization of molecules with low IPs, and the released electrons can be captured by electrophilic molecules to produce negative ions. Previously, Bruins and co-workers introduced a new LC/MS ionization method: dopant-assisted atmospheric pressure photoionization (DA-APPI) with acetone, toluene, or anisole as the dpants.[32,33] They found that the signals obtained for acabamazepine and acridines with toluene were at least 8 times as high as those obtained with APCI,[32] and the signals of 2-naphthol, anthracene, and diphenyl sulfide in acetonitrile obtained with anisole as dopant were about 100-fold higher than that obtained with toluene.[33] Moreover, the ionization mechanism in dopant-assisted APPI and the effect of solvent on ionization efficiency were also investigated.[34−36] In positive ion mode, the analytes were ionized either by charge exchange or by proton transfer. In negative ion mode, the products were formed via electron capture or by charge exchange processes. However, the investigation of a dopant-assisted negative photoionization source for ion mobility spectrometry was rare. In 2006, Nazarov et al. measured positive and negative ions using a miniature differential mobility spectrometer equipped with a photoionization source and detected sulfur hexafluoride and nitrogen oxides in negative mode with the addition of benzene or acetone as dopants to produce the electrons.[37] However, there is a lack of systematic study on the negative ionization source with addition of a dopant, such as the identification of reactant ions, the ionization mechanism, the stability, and the possibility for analysis explosives. In this article, we investigate in detail the capability of a dopant-assisted negative photoionization (DANP) source for ion mobility spectrometry using purified air as carrier and drift gases. The effects of dopant species and its concentration are investigated for a stable and strong reactant ion signal, and the stability and repeatability of DANP and UVRI are also compared. Then, the assignment of the reactant ion and its formation mechanism are discussed in detail. In the final section, the performances of DANP-IMS on detection of typical explosives are demonstrated.

EXPERIMENTAL SECTION

Apparatus. The schematic diagram of a homemade photoionization ion mobility spectrometer working in negative

dx.doi.org/10.1021/ac302836f | Anal. Chem. 2013, 85, 319−326

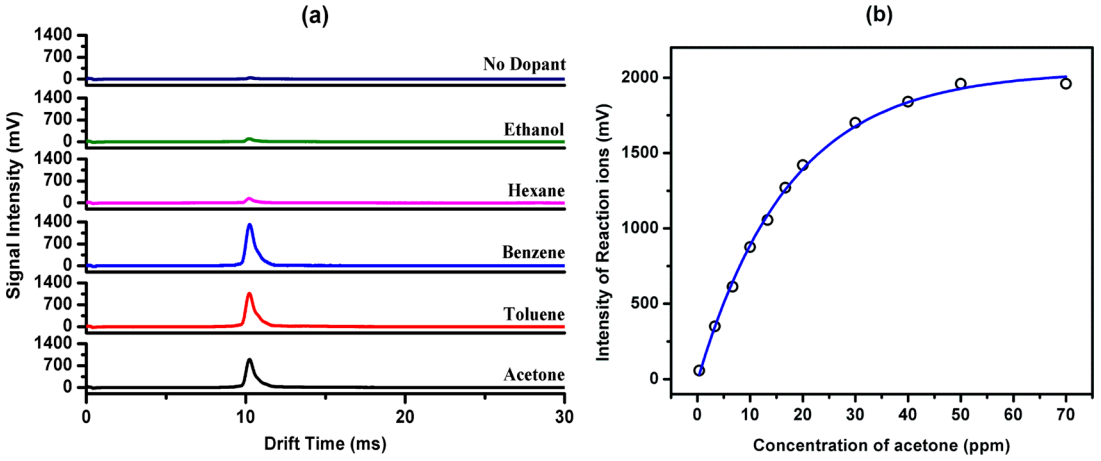

Figure 2. (a) Dopant-assisted negative photoionization ion mobility spectra of reactant ions with 10 ppm different compounds as dopant. (b) The evolution of the reactant ion intensity with acetone concentration at lamp current of 0.2 mA (black circle) and fitting line according to $I_e \propto I_0(1 - e^{-\sigma NL})$ (blue line).

mode is shown in Figure 1, which has been described previously,[30] except the metal grid in front of the lamp is removed. Here, only the main feature of the apparatus is outlined below. The IMS tube was constructed with a series of stacked stainless steel guard rings separated by Teflon insulating rings. The reaction region was 22 mm long with inner diameter 14 mm and the drift region was 88 mm long with inner diameter 30 mm. The guard rings were located 5.5 mm apart from each other and connected by a series of 1 MΩ resistors to form the electric gradient. The temperature of the IMS tube was kept at 90 °C. The ion gate was a Bradbury-Nielson type with an injection pulse width of 200 μs under current conditions. Ions were separated in the drift region and detected by the Faraday plate at the end of the drift tube. The ion current received by the Faraday plate was amplified with a gain of 10^9 V/A, and then fed to a computer via an A/D converter.

A commercial low-pressure dc-discharge Kr lamp (Cathodeon Ltd., Cambridge, UK) with MgF_2 window was used as the photoionization source to provide the ultraviolet photon with energy of 10.0 eV, and its working current was set at 0.2 mA. The voltage difference between the lamp and the extraction electrode was optimized at 1000 V to ensure the ion transmission efficiency. A homogeneous electrical field of 253.5 V/cm was maintained in the ion drift tube.

A bidirectional flow scheme was used in the IMS. The dopants in an 80 mL headspace sampling flask were carried into the photoionization chamber by carrier gas, and the drift gas was brought into the drift tube from the back of the Faraday plate to keep the drift tube free from contamination. The flow rates for carrier and drift gases were 400 and 600 mL/min, respectively. Solid explosives were directly carried into the ionization chamber of IMS by carrier gas through a thermal desorber, as shown in Figure 1. Both the carrier and drift gases were compressed air filtrated by activated carbon, silica gel, and freshly baked 13× molecular sieves trap; the moisture of the purified air was monitored by a dew point detector (DP300, CS Instrument GMH) and kept below 10 ppmv.

The reduced mobility values (K_0) for unknown peaks were calculated with a standard via the following equation:[38]

$$K_0^{\text{unknown}} = K_0^{\text{standard}} t_d^{\text{standard}} / t_d^{\text{unknown}} \quad (1)$$

where t_d^{standard} is the drift time for the standard, K_0^{standard} is the reduced mobility value for the standard, and t_d^{unknown} is the drift time for the interesting ion. $[TNT\text{-}H]^-$ produced in ^{63}Ni-IMS with air as carrier and drift gases was chosen as the standard due to its stable K_0 value (1.54 $cm^2\ V^{-1}\ s^{-1}$)[3] reported in literature.

Dopant and Sample Preparation Method. Acetone, benzene, toluene, *n*-hexane, and ethanol were all analytical grade and purchased from Kermel Chemicals Co., Ltd. (Tianjin, China). As dopant, these chemicals were placed inside a 2 mL vial (Agilent Technologies Co., Ltd.) sealed at one end by a porous capsule. The vial was place in an 80 mL flask and purified air was employed to purge the headspace of the flask to generate a carrier air flow with constant dopant concentration. The concentration of the dopant in the carrier gas could be controlled by adjusting the capsule and calculated by the weighting method.

Ammonium nitrate fuel oil explosive (ANFO), 2,4,6-trinitrotoluene (TNT), *N*-nitrobis(2-hydroxyethyl)amine dinitrate (DINA), and pentaerythritol tetranitrate (PETN) were all commercial grade. Stock solutions of 200 ng/μL were prepared by dissolving the appropriate quantity of these explosives in acetone. Explosive solutions of different concentration were obtained by successively diluting their stock solutions.

Sample Introduction System. The homemade thermal desorber was made of stainless steel and was controlled by an electromagnetic valve to open or close. The thermal desorber also equipped a heating plate and a digital temperature controller (AI-518, UDINA) and its temperature was kept at 160 °C. Five microliters of sample solution was first placed on a Teflon-coated fiberglass swab, and then inserted into the desorber after the solvent was evaporated. The dopant mixed carrier gas passed through the desorber and carried the sample vapor to the ionization chamber of the DANP-IMS for analysis.

RESULTS AND DISCUSSION

Effect of Dopant Species and Concentration. An ideal dopant for negative photoionization IMS should be simple to handle, efficient to ionize, and safe to use. Moreover, the formation of product ions of dopant in negative mode should be avoided and the spectra should be simple with the addition of dopants. Five common volatile compounds such as acetone (IE, 9.703 eV[39]), benzene (IE, 9.24 eV[39]), toluene (IE, 8.828

dx.doi.org/10.1021/ac302836f | Anal. Chem. 2013, 85, 319−326

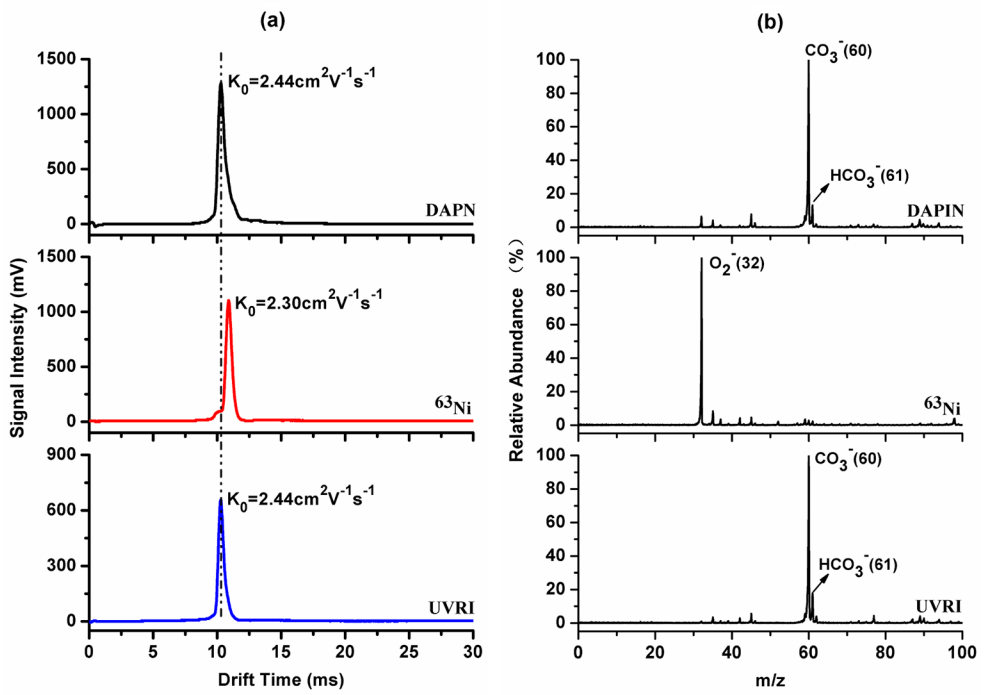

Figure 3. (a) Ion mobility spectra of purified air employing Dopant-assisted negative photoionization source, ^{63}Ni, and vacuum ultraviolet radiation induced[30] sources in negative mode. (b) Atmospheric pressure TOF mass spectrometry identification of reactant ions produced by ionization sources in part a.

eV[39]), ethanol (IE, 10.48 eV[39]), and *n*-hexane (IE, 10.13 eV[39]) had been tested as dopant, and their ion mobility spectra in negative mode obtained with 10 ppm concentration are shown in Figure 2a. The signal intensity observed in the ion mobility spectrum was only 40 mV without using dopant, which is ascribed to the formation of electron with the irradiation of extraction electrode by the VUV light. The intensity of reactant ions with 10 ppm ethanol, *n*-hexane, benzene, toluene, and acetone as dopant is 100, 145, 1300, 1000, and 900 mV, respectively, which is ascribed to their different photoionization cross sections.[40] It is noted that there is one dominant peak at drift time t_d = 10.24 ms (corresponding mobility of K_0 = 2.44 cm^2 V^{-1} s^{-1}) with a small tail on the right side in spite of five different dopants being used. Ethanol and *n*-hexane molecules were ruled out for a good dopant due to their low photoionization efficiency. Considering the toxicity of benzene and toluene, acetone was chosen as the dopant in the following experiments.

The production rate I_e (electron s^{-1}) of the electrons in a single photon ionization process can be expressed as follows:

$$I_e \propto I_0(1 - e^{-\sigma NL}) \quad (2)$$

where σ (Mb, 1 Mb = 10^{-18} cm^2) is the photoionization cross section of the dopant, I_0 (photons s^{-1}) is the photon flux of the lamp, N (cm^{-3}) is the molecular number density of the dopant, and L (cm) is the photoionization length. The amount of reactant ions in DANP source is proportional to the production rate of electrons. Figure 2b shows that the evolution of the measured intensity of reactant ion (black circle) with acetone concentration fits well with eq 2 (blue line) at a lamp current of 0.2 mA. In the low concentration range from 0.3 to 20 ppm, the signal intensity of reactant ions increases almost linearly. Then, the intensity of reactant ions increases slowly and reaches a statured response after the acetone concentration is higher than 30 ppm. Overfull dopant would not produce more reactant ions, but causes high consumption of the dopant and shortens its service time. So in the following experiments, 20 ppm of acetone was used as the dopant in the DANP ion mobility spectrometry, which can provide enough reactant ions and avoid excess consumption of acetone.

Identification of Reactant Ions in DANP Ion Mobility Spectrometry. What is the reactant ion in the DANP source? First, we compared the RIPs in DANP, ^{63}Ni, and UVRI sources in negative mode. Figure 3a shows the ion mobility spectra obtained by DANP, ^{63}Ni, and UVRI sources with purified air as the carrier and the drift gases, in which all the experimental parameters were kept the same except for the ionization source. The DANP source and UVRI source produced a dominant ion peak with a corresponding K_0 value of 2.44 cm^2 V^{-1} s^{-1}, while the ^{63}Ni source formed ions with a corresponding K_0 value of 2.30 cm^2 V^{-1} s^{-1}, which implies that the reactant ions in DANP source and UVRI photoemission source may be the same but different from those in ^{63}Ni source.

To identify the chemical composition of the reactant ions in DANP, UVRI, and ^{63}Ni sources, the ions were analyzed by a homemade atmospheric pressure time-of-flight (TOF) mass spectrometer (see Figure-S1 in the Supporting Information), and the typical mass spectra are displayed in Figure 3b. In DANP and UVRI sources, the ions with *m*/*z* 60 were the predominant ions, which have two possible assignments, $N_2O_2^-$ or CO_3^-. However, in ^{63}Ni source, the reactant ions are dominated by the ions with *m*/*z* 32, which is identified as O_2^- and is consistent with the previous study by Waltman et al.[41] The ions at *m*/*z* 60 were also observed in negative corona discharge source.[42,43] Sabo et al. ascribed the ions at *m*/*z* 60 to be $N_2O_2^-$ when the water and carbon dioxide in high-purity oxygen was as low as subppb levels.[42] But Ewing et al. confirmed the ions at *m*/*z* 60 ion as CO_3^- even when CO_2

dx.doi.org/10.1021/ac302836f | *Anal. Chem.* 2013, 85, 319−326

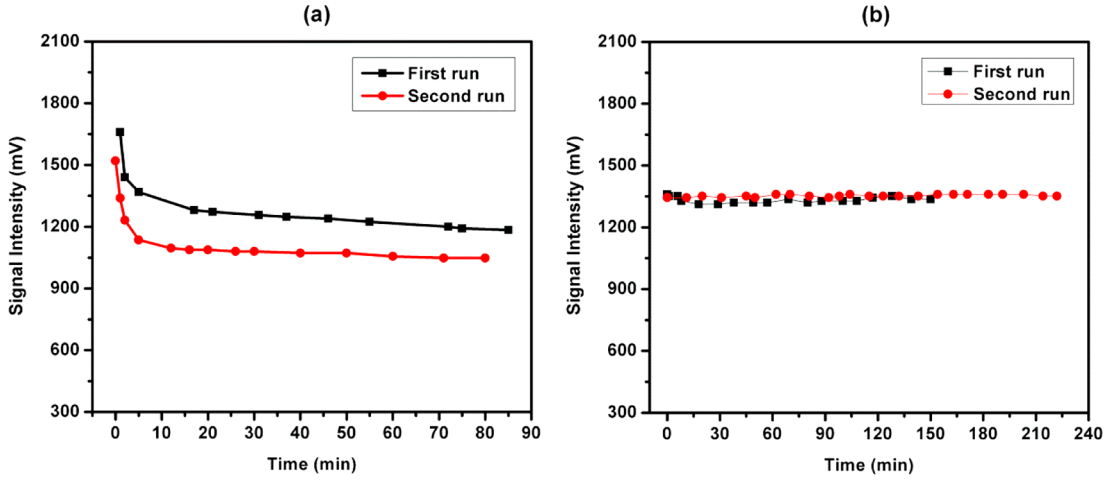

Figure 4. The intensity of reactant ions vs time for vacuum ultraviolet radiation induced negative ionization source[30] (a) and dopant-assisted negative photoionization source with 20 ppm acetone as the dopant (b).

presented in low ppmv level through the use of ^{18}O labeled oxygen technique.[43] In our system, the measured concentration of CO_2 in purified air was about 300 ppm by electron impact ionization time-of-flight mass spectrometry,[44] so the ions at m/z 60 in DANP and UVRI sources are assigned to CO_3^-.

The formation mechanism of the reactant ions in DANP source will be discussed below. In the ionization region of DANP-IMS, low-energy electrons were produced by VUV photoionization of dopant agent. Simultaneously, O_3 was also generated due to the high concentration of O_2 molecules, large photoabsorption cross section of O_2 molecules at 123.5 nm, and the low heat of formation for ozone (34.1 kcal/mol).[45] The O_3 concentration in DANP source was about 1700 ppm measured by using the iodometric titration method.

$$\text{dopant} + h\nu \rightarrow e^- \quad (3)$$

$$O_2 + h\nu \rightarrow O + O \quad (4)$$

$$O + O_2 \rightarrow O_3 \quad (5)$$

Then, the O_3 and O_2 molecules in the ionization region could capture the low-energy electron and form O_3^- and O_2^- ions, which would further cluster water molecules to form their hydrated anions under ambient pressure. Besides, a part of hydrated O_3^- could be transformed from $O_2^-(H_2O)_n$ through charge-transfer reaction 10.

$$e^- + O_2 + M \rightarrow O_2^- + M\ (M = N_2, O_2, H_2O, \text{etc.}) \quad (6)$$

$$e^- + O_3 + M \rightarrow O_3^- + M \quad (7)$$

$$O_2^- + nH_2O + M \rightarrow O_2^-(H_2O)_n + M \quad (8)$$

$$O_3^- + nH_2O + M \rightarrow O_3^-(H_2O)_n + M \quad (9)$$

$$O_2^-(H_2O)_n + O_3 \rightarrow O_3^-(H_2O)_m + O_2 + (n-m)H_2O \quad (10)$$

As there is about 300 ppm CO_2 present in the carrier gas, the hydrated O_3^- ions could convert to hydrated CO_3^- ions in only about 0.4 μs due to the negative Gibbs free energy of reaction 11 (<−8.3 kcal/mol) and its rate constant $k = 5.5 \times 10^{-10}$ cm^3/s.[46]

$$O_3^-(H_2O)_n + CO_2 \rightarrow CO_3^-(H_2O)_m + (n-m)H_2O + O_2 \quad (11)$$

It is noted that only core ions were observed in mass spectra of reactant ions, the cluster ions formed in the ionization source could be declustered when they pass the skimmer of the source chamber to the lower pressure chamber of mass spectrometer.

The Stability of DANP Ion Mobility Spectrometry. The stability of RIP in IMS is important for quantitative analysis and reducing the false rate for on-site detection. Figure 4 shows the evolution of signal intensity of reactant ions as a function of operational time for UVRI and DANP sources. As shown in Figure 4a, the signal intensity of reactant ions in UVRI source decays more than 20% in the first 10 min, then reaches a relatively stable signal intensity with variation of 40−60 mV (less than 5%) every hour when increasing the operational time. This phenomenon was also noted by Ewing et al. in recent investigation of photoemission ambient pressure ionization applied in mass spectrometry.[47] Besides the turn-on rapid decay of reactant ion intensity, the reproducibility of the RIP intensity is poor between different run times. One possible explanation for the decay is the contamination (oxidation or coating) of the photocathode surface upon exposure to UV light, which may inhibit electron emission. For DANP source, as shown in Figure 4b, excellent stability and reproducibility of RIP were acquired, the relative standard deviations of the RIP intensities for the first run (150 min) and second run (220 min) were 0.5% and 0.15%, respectively. Compared to UVRI, the dopant assisted photoionization source could achieve much better turn-on reproducibility and stability.

Detection of Explosives with DANP Ion Mobility Spectrometry. Ion mobility spectrometry has become the most popular and widely used on-site instrument for detection of trace level explosives in the last decades. The performances of DANP ion mobility spectrometry for explosive detection were investigated in this section. The DANP ion mobility spectra of 10 ng of ANFO, 10 ng of TNT, 10 ng of DINA, and 10 ng of PETN are shown in Figure 5. It is clear that these explosives could be sensitively detected with S/N better than hundreds. And more, only one dominant product ion peak is formed for each single explosive compound, which is a benefit for explosives identification in complex environments. Product ions of each explosive compound were analyzed by atmospheric

dx.doi.org/10.1021/ac302836f | Anal. Chem. 2013, 85, 319−326

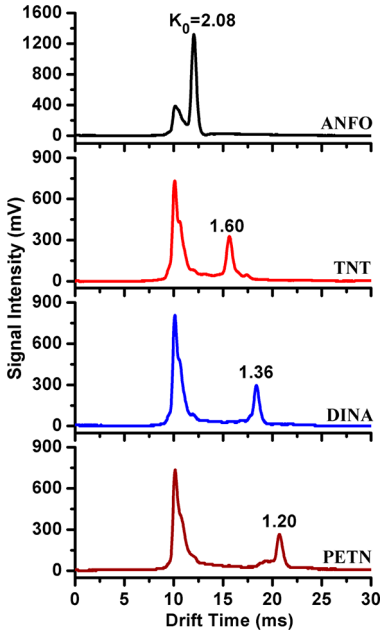

Figure 5. Ion mobility spectra of 10 ng of ANFO, 10 ng of TNT, 10 ng of DINA, and 10 ng of PETN obtained by the dopant-assisted negative photoionization source ion mobility spectrometer with 20 ppm acetone as the dopant.

pressure TOF mass spectrometer and the corresponding mass spectra are shown in Figure 6. For ANFO, CO_3^- at m/z 60, NO_3^- at m/z 62, and $HNO_3{\cdot}NO_3^-$ at m/z 125 were observed in the mass spectrum shown in Figure 6a. The reduced mobility for ANFO product ions is 2.08 $cm^2\ V^{-1}\ s^{-1}$, which agrees very well with the K_0 value of $HNO_3{\cdot}NO_3^-$ of 2.08 $cm^2\ V^{-1}\ s^{-1}$ reported by Kozole et al.[48] $HNO_3{\cdot}NO_3^-$ may be formed via decomposition of NH_4NO_3 (the main component of ANFO) to form HNO_3 followed by ion-association reaction with NO_3^-, the NO_3^- is generated from HNO_3 via hydrogen abstraction reaction with CO_3^- ions. Appearance of NO_3^- in the mass spectra may be due to the pressure difference between ion mobility spectrometry and mass spectrometry. Compared with ^{63}Ni source, the separation between the DANP reactant ions and $HNO_3{\cdot}NO_3^-$ is larger, which can avoid the interference from the tail of reactant ions, and makes the detection of low concentration ANFO possible. For PETN, product ions with reduced mobility of 1.20 $cm^2\ V^{-1}\ s^{-1}$ in DANP-IMS, which is close to the value of 1.18 $cm^2\ V^{-1}\ s^{-1}$ in ^{63}Ni-IMS reported by Kozole et al.,[49] are assigned to a mixture of $PETN{\cdot}CO_3^-$ (m/z 376) and $PETN{\cdot}NO_3^-$ (m/z 378) as shown in Figure 6d. The mass spectra results clearly indicate that PETN could be directly ionized by association reaction with the reactant ions CO_3^- in DANP source. Similar to PETN, product ions of DINA with reduced mobility 1.36 $cm^2\ V^{-1}\ s^{-1}$ also include both $DINA{\cdot}CO_3^-$ (m/z 300) and $DINA{\cdot}NO_3^-$ (m/z 302) as shown in Figure 6c. The production of NO_3^- ions in the detection of PETN and DAIN may come from dissociative ionization of PETN and DIAN molecules. Different from ANFO, PETN, and DINA, the reduced mobility of product ions for TNT in DANP-IMS is 1.60 $cm^2\ V^{-1}\ s^{-1}$, which is obviously different from the value of 1.54 $cm^2\ V^{-1}\ s^{-1}$ for $[TNT\text{-}H]^-$ in ^{63}Ni-IMS as shown in Figure S-2a (Supporting Information). In the mass spectrum of TNT, ions at m/z 197 and m/z 213 appear besides ions at m/z 226 in DANP-IMS compared with ^{63}Ni-IMS (Figure S-2b, Supporting Information). The ions at m/z 197 and m/z 213 are ascribed to $[TNT\text{-}NO]^-$ and $[TNT\text{-}CH_2]^-$, which are formed due to the presence of UV light and/or O_3 in DANP source.

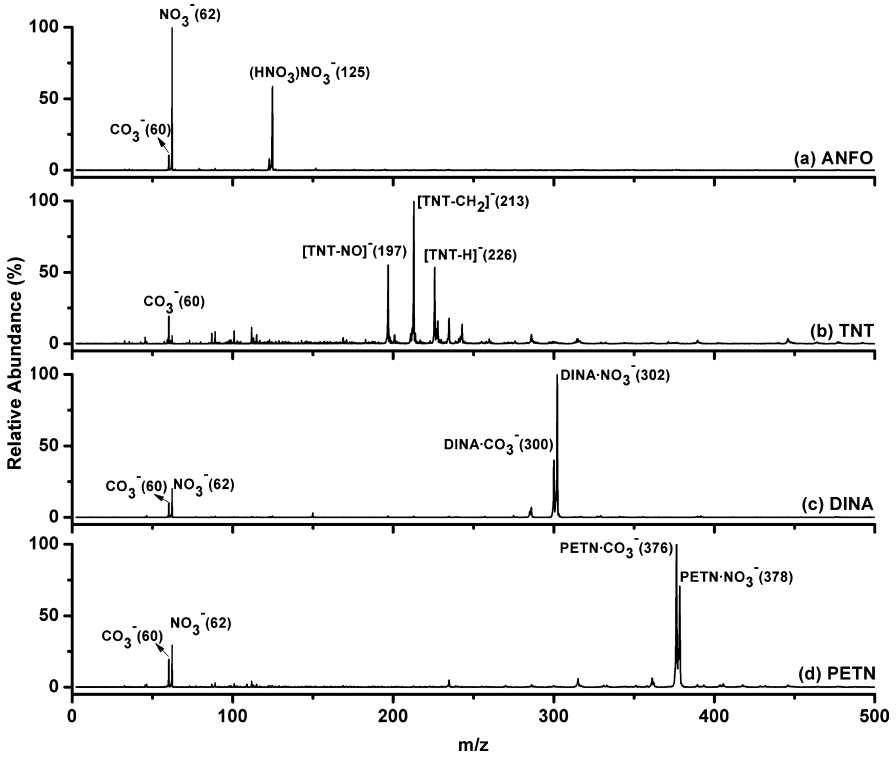

Figure 6. Mass spectra of product ions for explosives (a) ANFO, (b) TNT, (c) DINA, and (d) PETN in dopant-assisted negative photoionization source obtained by TOF mass spectrometry.

dx.doi.org/10.1021/ac302836f | Anal. Chem. 2013, 85, 319−326

The responses of DANP-IMS against the amount of explosives for ANFO, TNT, and DINA were evaluated and the results are shown in Figure 7. The working ranges were

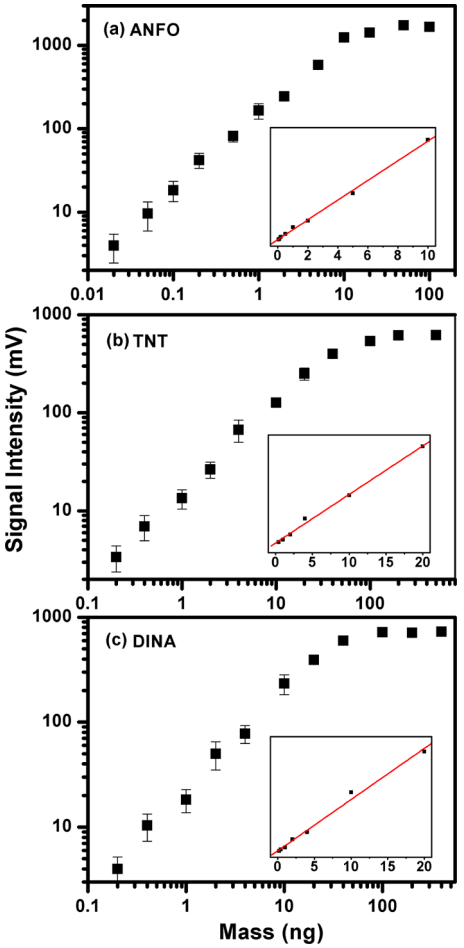

Figure 7. Response curve (log/log) and linear calibration curve (inset plot) for ANFO, TNT, and DINA with 20 ppm acetone as the dopant in DANP ion mobility spectrometry. Three orders of magnitude for response range and 2 orders of magnitude for linear range were achieved.

0.02−10, 0.2−100, and 0.2−100 ng for ANFO, TNT, and DINA, respectively. The corresponding linear calibration ranges, shown in the inset plots, were 0.05−10, 0.4−20, and 0.2−20 ng, respectively. It can be seen that the working ranges are about 3 orders of magnitude and the linear ranges are about 2 orders of magnitude. Their calculated limits of detection (LOD) (S/N = 3) are 10, 80, and 100 pg for ANFO, TNT, and DINA, respectively. These results exhibit a good quantitative capability of DANP ion mobility spectrometry for explosive detection.

CONCLUSION

A simple, stable, and efficient nonradioactive DANP ionization source has been developed and tested, which used a commercial VUV krypton lamp to ionize volatile compounds, such as acetone or toluene, as the source of electrons to produce negative reactant ions. With 20 ppm of acetone as the dopant, single reactant ion peak was formed with reduced mobility of $K_0 = 2.44\ cm^2\ V^{-1}\ s^{-1}$ when using dry purified air as carrier and drift gases. The reactant ions formed in DANP source were predominantly assigned to hydrated CO_3^- ions based on the measured m/z by an atmospheric pressure TOF mass spectrometer. The relative standard deviation of reactant ion intensity for reactant ions peak was smaller than 0.5% for operating 150 min. Preliminary application in detection of common explosives showed excellent qualitative capacity and good sensitivity, for example, only one dominant product ion peak was formed in IMS for ANFO, TNT, DINA, and PETN, and the LODs of 10 (ANFO), 80 (TNT), and 100 pg (DINA) with a linear range of 2 orders of magnitude were achieved. The time-of-flight mass spectra obtained by using DANP source clearly indicated that PETN and DINA can be directly ionized by the ion-association reaction of CO_3^- to form PETN·CO_3^- and DINA·CO_3^- adduct ions, which result in good sensitivity for the DANP source. It should be noted that the presence of VUV light and/or high concentration O_3 in DANP source can cause additional reactions for TNT, which results in the formation of $[TNT\text{-}NO]^-$ and $[TNT\text{-}CH_2]^-$.

ASSOCIATED CONTENT

Supporting Information

Schematic diagram of the MS instrument and Ion mobility spectra of TNT and mass spectra of product ions for TNT. This material is available free of charge via the Internet at http://pubs.acs.org.

AUTHOR INFORMATION

Corresponding Author

*E-mail: hli@dicp.ac.cn. Fax: +86-411-84379517.

Notes

The authors declare no competing financial interest.

ACKNOWLEDGMENTS

This work is partially supported by the National Special Fund for the Development of Major Research Equipment and Instrument (Grants 2011YQ05006903 and 2011YQ05006904), 863 Plan (Grant 2011AA060602), NSF of China (Grants 11004190, 21177124, 21077101, 20907052, 21177124, 21275143, and 21207129), Instrument Developing Project of the Chinese Academy of Sciences (Grant YZ200907), NSF of Liaoning Province (Grant 201102220), and Science and Technology Plan Project of Dalian City (Grant 2010J21DW028).

REFERENCES

(1) Eiceman, G. A.; Karpas, Z. *Ion Mobility Spectrometry*, 2nd ed.; CRC Press: Boca Raton, FL, 2005.
(2) Borsdorf, H.; Eiceman, G. A. *Appl. Spectrosc. Rev.* **2006**, *41*, 323−375.
(3) Ewing, R. G.; Eiceman, G. A.; Atkinson, D. A.; Ewing, G. J. *Talanta* **2001**, *54*, 515−529.
(4) Schmidt, H.; Sielemann, S. *Spectrochim. Acta, Part B* **2002**, *57*, 1563−1574.
(5) Khayamian, T.; Tabrizchi, M.; Jafari, M. T. *Talanta* **2006**, *69*, 795−799.
(6) Steiner, W. E.; Clowers, B. H.; Haigh, P. E.; Hill, H. H. *Anal. Chem.* **2003**, *75*, 6068−6076.
(7) Sielemann, S.; Zhiyong, X.; Schmidt, H. *Anal. Chem.* **2003**, *75*, 1483−1490.
(8) Kanu, A. B.; Hill, H. H. *J. Chromatogr., A* **2008**, *1177*, 12−27.
(9) Balm, M. A.; Hill, H. H. *Anal. Chem.* **1982**, *54*, 38−43.
(10) Karpas, Z.; Wang, Y. F.; Eiceman, G. A. *Anal. Chim. Acta* **1993**, *282*, 19−31.

(11) Simpson, G.; Klasmeier, M.; Hill, H. H.; Atkinson, D.; Radolovich, G.; Lopez-Avila, V.; Jones, T. L. *J. High Resolut. Chromatogr.* **1996**, *19*, 301−312.
(12) Eckers, C.; Laures, A.M.-F.; Giles, K.; Major, H.; Pringle, S. *Rapid Commun. Mass Spectrom.* **2007**, *21*, 1255−1263.
(13) Baim, M. A.; Eatherton, R. L.; Hill, H. H. *Anal. Chem.* **1983**, *55*, 1761−1766.
(14) Leasure, C. S.; Fleischer, M. E.; Anderson, G. K.; Eiceman, G. A. *Anal. Chem.* **1986**, *58*, 2142−2147.
(15) Baumbach, J. I.; Sielemann, S.; Xie, Z. Y.; Schmidt, H. *Anal. Chem.* **2003**, *75*, 1483−1490.
(16) Bahrami, H.; Tabrizchi, M. *Talanta* **2012**, *97*, 400−405.
(17) Tabrizchi, M.; Khayamian, T.; Taj, N. *Rev. Sci. Instrum.* **2000**, *71*, 2321−2328.
(18) Ewing, R. G.; Waltman, M. J. *Int. J. Ion Mobility Spectrom.* **2009**, *12*, 65−72.
(19) Tabrizchi, M.; Jazan, E. *Anal. Chem.* **2010**, *82*, 746−750.
(20) Roscioli, K. M.; Davis, E.; Siems, W. F.; Maariano, A.; Su, W. S.; Guharay, S. K.; Hill, H. H. *Anal. Chem.* **2011**, *83*, 5965−5971.
(21) Chen, Y. H.; Luckenblll, W. K.; Hill, H. H. *Anal. Chem.* **1994**, *66*, 2348−2355.
(22) Tam, M.; Hill, H. H. *Anal. Chem.* **2004**, *76*, 2741−2747.
(23) Khayamian, T.; Jafari, M. T. *Anal. Chem.* **2007**, *79*, 3199−3205.
(24) Jafari, M. T.; Javaheri, M. *Anal. Chem.* **2010**, *82*, 6721−6725.
(25) Andrade, F. J.; Shelley, J. T.; Wetzel, W. C.; Webb, M. R.; Gamez, G.; Ray, S. J.; Hieftje, G. M. *Anal. Chem.* **2008**, *80*, 2654−2663.
(26) Dong, C.; Wang, W.; Li, H. *Anal. Chem.* **2008**, *80*, 3925−3930.
(27) Sielemann, S.; Baumbach, J. I.; Pilzecker, P.; Walendzik, G. *Int. J. Ion Mobility Spectrom.* **1999**, *2*, 15−21.
(28) Begley, P.; Corbin, R.; Foulger, B. E.; Simmonds, P. G. *J. Chromatogr.* **1991**, *588*, 239−249.
(29) Walls, C. J.; Swenson, O. F.; Gillispie, G. D. *Proc. SPIE* **1999**, *3534*, 290−298.
(30) Chen, C.; Dong, C.; Du, Y. Z.; Cheng, S. S.; Han, F. L.; Li, L.; Wang, W. G.; Hou, K. Y.; Li, H. Y. *Anal. Chem.* **2010**, *82*, 4151−4157.
(31) Bunker, S. N.; Krasnobaev, L.; Framingham, M. A. Patent No.: 7576320B2.
(32) Robb, D. B.; Covey, T. R.; Bruins, A. P. *Anal. Chem.* **2000**, *72*, 3653−3659.
(33) Kauppila, T. J.; Kostiainen, R.; Bruins, A. P. *Rapid Commun. Mass Spectrom.* **2004**, *18* (7), 808−815.
(34) Kauppila, T. J.; Kuuranne, T.; Meurer, E. C.; Eberlin, M. N.; Kotiaho, T.; Kostiainen, R. *Anal. Chem.* **2002**, *74*, 5470−5479.
(35) Kauppila, T. J.; Kotiaho, T.; Kostiainen, R. *J. Am. Soc. Mass Spectrom.* **2004**, *15* (2), 203−211.
(36) Song, L. G.; Wellman, A. D.; Yao, H. F.; Bartmess, J. E. *J. Am. Soc. Mass Spectrom.* **2007**, *17*, 1789−1798.
(37) Nazarov, E. G.; Miller, R. A.; Eiceman, G. A.; Stone, J. A. *Anal. Chem.* **2006**, *78*, 4553−4563.
(38) Eiceman, G. A.; Nazarov, E. G.; Stone, J. A. *Anal. Chim. Acta* **2003**, *493*, 185−194.
(39) http://webbook.nist.gov/chemistry/
(40) Adam, T.; Zimmermann, R. *Anal. Bioanal. Chem.* **2007**, *389*, 1941−1951.
(41) Waltman, M. J.; Dwivedi, P.; Hill, H. H.; Blanchard, W. C.; Ewing, R. G. *Talanta* **2008**, *77*, 249−255.
(42) Sabo, M.; Palenik, J.; Kucera, M.; Han, H. Y.; Wang, H. M.; Chu, Y. N.; Matejcik, S. *Int. J. Mass Spetrom.* **2010**, *293*, 23−27.
(43) Ewing, R. G.; Waltman, M. J. *Int. J. Mass Spectrom.* **2010**, *296*, 53−58.
(44) Wu, Q. H.; Hua, L.; Hou, K. Y.; Cui, H. P.; Chen, W. D.; Chen, P.; Wang, W. G.; Li, J. H.; Li, H. Y. *Anal. Chem.* **2011**, *83*, 8992−8998.
(45) Lide, D. R. *CRC Handbook of Chemistry and Physics*; CRC Press: Boca Raton, FL, 2010.
(46) Fehsenfeld, F. C.; Ferguson, E. E. *J. Chem. Phys.* **1974**, *61*, 3181−3193.
(47) Short, L. C.; Ewing, R. G.; Barinaga, C. J. *Rapid Commun. Mass Spectrom.* **2011**, *25*, 2888−2896.
(48) Kozole, J.; Tomlinson-Phillips, J.; Stairs, J. R.; Harper, J. D.; Lukow, S. R.; Lareau, R. T.; Boudries, H.; Lai, H.; Brauer, C. S. *Talanta* **2012**, *99*, 799−810.
(49) Kozole, J.; Stairs, J. R.; Cho, I.; Harper, J. D.; Lukow, S. R.; Lareau, R. T.; DeBono, R.; Kuja, F. *Anal. Chem.* **2011**, *83*, 8596−8603.